Acknowledgements

This study was supported, in part, by a grant-in-aid for Scientific Research (No. 19790513, 20590813, 21790701) from the Ministry of Education Culture, Sport, Science and Technology and a grant-in-aid from the global century center of excellence (COE) program of the Japan Society for the Promotion of Science. We would like to thank Mr. Akio Okada for his technical supports.

References

1. Eisenhofer G, Friberg P, Rundqvist B, Quyyumi AA, Lambert G, Kaye DM, et al. Cardiac sympathetic nerve function in congestive heart failure. Circulation 1996;93:1667-76.

2. Rundqvist B, Elam M, Bergmann-Sverrisdottir Y, Eisenhofer G, Friberg P. Increased cardiac adrenergic drive precedes generalized sympathetic activation in human heart failure. Circulation 1997;95:169-75.

3. Packer M. The neurohormonal hypothesis: a theory to explain the mechanism of disease progression in heart failure. J Am Coll Cardiol 1992;20:248-54.

4. Cohn JN, Levine TB, Olivari MT, Garberg V, Lura D, Francis GS, et al. Plasma norepinephrine as aguide to prognosis in patients with chronic congestive heart failure. N Engl J Med 1984;311:819-23.

5. Rector TS, Olivari MT, Levine TB, Francis GS, Cohn JN. Predicting survival for an individual with congestive heart failure using the plasma norepinephrine concentration. Am Heart J 1987;114:148-52.

6. Heilbrunn SM, Shah P, Bristow MR, Valantine HA, Ginsburg R, Fowler MB. Increased β -receptor density and improved hemodynamic response to catecholamine stimulation during long-term metoprolol therapy in heart failure from dilated cardiomyopathy. Circulation 1989;79:483-90.

7. Nakata T, Miyamoto K, Doi A, Sasao H, Wakabayashi T, Kobayashi H, et al. Cardiac death

prediction and impaired cardiac sympathetic innervations assessed by MIBG in patients with failing and nonfailing hearts. J Nucl Cardiol 1998;5:579-90.

8. Imamura Y, Ando H, Mitsuoka W, Egashira S, Masaki H, Ashihara T, et al. Iodine-123 metaiodobenzylguanidine images reflect intense myocardial adrenergic nervous activity in congestive heart failure independent of underlying cause. J Am Coll Cardiol 1995;26:1594-9.
9. Arimoto T, Takeishi Y, Fukui A, Tachibana H, Nozaki N, Hirono O, et al. Dynamic ^{123}I-MIBG SPECT reflects sympathetic nervous integrity and predicts clinical outcome in patients with chronic heart failure. Ann Nucl Med 2004;18:145-50.
10. Arimoto T, Takeishi Y, Niizeki T, Nozaki N, Hirono O, Watanabe T, et al. Cardiac sympathetic denervation and ongoing myocardial damage for prognosis in early stages of heart failure. J Card Fail 2007;13:34-41.
11. Agostini D, Carrio I, Verberne HJ. How to use myocardial 123I-MIBG scintigraphy in chronic heart failure. Eur J Nucl Med Mol Imaging 2009;36:555-59.
12. Redfield MM, Jacobsen SJ, Burnett JC Jr, Mahoney DW, Bailey KR, Rodeheffer RJ. Burden of systolic and diastolic ventricular dysfunction in the community: appreciating the scope of the heart failure epidemic. JAMA 2003;289:194-202.
13. Vasan RS, Larson MG, Benjamin EJ, Evans JC, Reiss CK, Levy D. Congestive heart failure in subjects with normal versus reduced left ventricular ejection fraction: prevalence and mortality in a population-based cohort. J Am Coll Cardiol 1999;33:1948-55.

14. Yusuf S, Pfeffer MA, Swedberg K, Granger CB, Held P, McMurray JJ, et al; CHARM Investigators and Committees. Effects of candesartan in patients with chronic heart failure and preserved left-ventricular ejection fraction: the CHARM-Preserved trial. Lancet 2003;362:777-81.

15. Kitahara T, Takeishi Y, Arimoto T, Niizeki T, Koyama Y, Sasaki T, et al. Serum carboxy-terminal telopeptide of type I collagen (ICTP) predicts cardiac events in chronic heart failure patients with preserved left ventricular systolic function. Circ J 2007;71:929-35.

16. Sugiura M, Yamamoto K, Takeda Y, Takeda Y, Dohmori T, Ogata M, et al. The relationship between variables of 123-I-metaiodobenzylguanidine cardiac imaging and clinical status of the patients with diastolic heart failure. Int J cardiol 2006;113:223-228.

17. Tsuchihashi-Makaya M, Hamaguchi S, Kinugawa S, Yokota T, Goto D, Yokoshiki H, et al. Characteristics and outcomes of hospitalized patients with heart failure and reduced vs preserved ejection fraction. Report From the Japanese Cardiac Registry of Heart Failure in Cardiology (JCARE-CARD). Circ J 2009;73:1893-1900.

18. Borlaug BA, Melenovsky V, Russell SD, Kessler K, Pacak K, Becker LC, Kass DA. Impaired chronotropic and vasodilator reserves limit exercise capacity in patients with heart failure and a preserved ejection fraction. Circulation 2006;114:2138-2147.

19. Arimoto T, Takeishi Y, Shiga R, Fukui A, Tachibana H, Nozaki N, et al. Prognostic value of elevated circulating heart-type fatty acid binding protein in patients with congestive heart failure.

J Card Fail 2005;11:56-60.

20. Niizeki T, Takeishi Y, Watanabe T, Nitobe J, Miyashita T, Miyamoto T, et al. Relation of serum heat shock protein 60 level to severity and prognosis in chronic heart failure secondary to ischemic or idiopathic dilated cardiomyopathy. Am J Cardiol 2008;102:606-10.

21. Estorch M, Carrió I, Mena E, Flotats A, Camacho V, Fuertes J, et al. Challenging the neuronal MIBG uptake by pharmacological intervention: effect of a single dose of oral amitriptyline on regional cardiac MIBG uptake. Eur J Nucl Med Mol Imaging 2004;31:1575-80.

22. Niizeki T, Takeishi Y, Arimoto T, Takahashi T, Okuyama H, Takabatake N, et al. Combination of heart-type fatty acid binding protein and brain natriuretic peptide can reliably risk stratify patients hospitalized for chronic heart failure. Circ J 2005;69:922-27.

23. Arimoto T, Takeishi Y, Niizeki T, Takabatake N, Okuyama H, Fukui A, et al. Cyctatin C is a novel predictor of cardiac events in patients with chronic heart failure. J Card Fail 2005;11:595-601.

24. Suzuki S, Takeishi Y, Niizeki T, Koyama Y, Kitahara T, Sasaki T, et al. Pentraxin 3, a new marker for vascular inflammation, predicts adverse clinical outcomes in patients with heart failure. Am Heart J 2008;155:75-81.

25. Niizeki T, Takeishi Y, Arimoto T, Takabatake N, Nozaki N, Hirono O, et al. Heart-type fatty acid-binding protein is more sensitive than troponin T to detect the ongoing myocardial damage in chronic heart failure patients. J Card Fail 2007;13:120-27.

26. Takeishi Y, Atsumi H, Fujiwara S, Takahashi K, Tomoike H. ACE inhibition reduces cardiac iodine-123-MIBG release in heart failure. J Nucl Med 1997;38:1085-9.

27. Atsumi H, Takeishi Y, Fujiwara S, Tomoike H. Cardiac sympathetic nervous disintegrity is related to exercise intolerance in patients with chronic heart failure. Nucl Med Commun 1998;19:451-6.

28. Matsuo S, Imai E, Horio M, Yasuda Y, Tomita K, Nitta K, et al; Collaborators developing the Japanese equation for estimated GFR. Revised equations for estimated GFR from serum creatinine in Japan. Am J Kidney Dis 2009;53:982-92.

29. Grassi G, Seravalle G, Quarti-Trevano F, Dell'Oro R, Bolla G, Mancia G. Effects of hypertension and obesity on the sympathetic activation of heart failure patients. Hypertension 2003;42:873-877.

30. Kitzman DW, Brubaker PH, Anderson RT, Brosnihan B, Stewart KP, Welsley DJ, et al. Isolated diastolic heart failure: Does it exist? Characterization of an important syndrome among the elderly. J Am Coll Cardiol 2000;35:193A.

31. Kaneko N, Matsuda R, Nakajima T, Shinozaki M, Ohtani N, Oda K, et al. Norepinephrine-induced diastolic dysfunction with aortic valve opening under calcium-loading in rats. Drug Dev Res;2006:67:511-518.

32. Deten A, Shibata J, Scholz D, Briest W, Wagner KF, Wenger RH, et al. Norepinephrine –induced acute heart failure in transgenic mice overexpressing erythropoietin. Cardiovasc Res

2004;61:105-114.

33. Lorell BH, Grossman W. Cardiac hypertrophy: the consequences for diastole. J Am Coll Cardiol 1987;9:1189-1193.

34. Levi R, Silver RB, Mackins CJ, Seyedi N, Koyama M. Activation of a renin-angiotensin system in ischemic cardiac sympathetic nerve endings and its association with norepinephrine release. Int Immunopharmacol 2002;2:1965-1973.

35. Isobe S, Izawa H, Iwase M, Nanasato M, Nonokawa M, Ando A, et al. Cardiac ^{123}I-MIBG reflects left ventricular functional reserve in patients with nonobstructive hypertrophic cardiomyopathy. J Nucl Med 2005;46:909-16.

36. Kasama S, Toyama T, Kumakura H, Takayama Y, Ichikawa S, Suzuki T, et al. Effects of candesartan on cardiac sympathetic nerve activity in patients with congestive heart failure and preserved left ventricular ejection fraction. J Am Coll Cardiol. 2005;45:661-7.

37. Grewal J, McKelvie RS, Persson H, Tait P, Carlsson J, Swedberg K, et al. Usefulness of N-terminal pro-brain natriuretic peptide and brain natriuretic peptide to predict cardiovascular outcomes in patients with heart failure and preserved left ventricular ejection fraction. Am J Cardiol 2008;102:733-7.

38. Yoshimura M, Yasue H, Okumura K, Ogawa H, Jougasaki M, Mukoyama M, et al. Different secretion patterns of atrial natriuretic peptide and brain natriuretic peptide in patients with congestive heart failure. Circulation 1993;87:464-9.

39. Forfia PR, Watkins SP, Rame JE, Stewart KJ, Shapiro EP. Relationship between B-type natriuretic peptides and pulmonary capillary wedge pressure in the intensive care unit. J Am Coll Cardiol 2005;45:1667-71.

40. Yamamoto K, Nishimura RA, Chaliki HP, Appleton CP, Holmes DR Jr, Redfield MM. Determination of left ventricular filling pressure by Doppler echocardiography in patients with coronary artery disease: critical role of left ventricular systolic function. J Am Coll Cardiol 1997;30:1819-26.

Figure legends

Figure 1. Delayed H/M ratio of ^{123}I-MIBG (a) and washout rate (b) in the study population.

Figure 2. Relationships between the washout rate of ^{123}I-MIBG and the plasma level of BNP (a), and the echocardiographic LVEF (b).

Figure 3. Washout rate of ^{123}I-MIBG and all cardiac events of patients with heart failure with preserved ejection fraction. Survival curves were created by a Kaplan-Meier method and analyzed by a log-rank test.

Table 1. Clinical characteristics of control subjects and 94 patients with heart failure

	Control n = 20	HFPEF n = 94	p Value
Age (y)	57 ± 17	64 ± 15	0.0438
Gender (male/female)	10/10	54/40	NS
NYHA functional Class (I/II/III/IV)	-	26/51/17/0	-
Hypertension	5 (25%)	48 (51%)	0.0274
Hyperlipidemia	4 (20%)	17 (18%)	NS
Diabetes mellitus	4 (20%)	17 (18%)	NS
Current smoker	3 (15%)	19 (20%)	NS
Etiology			
Dilated cardiomyopathy	-	19 (20%)	-
Ischemic heart failure	-	14 (15%)	-
Valvular heart disease	-	23 (24%)	-
Hypertensive heart disease	-	6 (6%)	-
Arrhythmogenic	-	17 (18%)	-
Others	-	15 (16%)	-
Blood examination			
Sodium (mEq/L)	142 ± 2.0	141 ± 3.0	NS
Uric acid (mg/dL)	4.7 ± 1.1	6.1 ± 2.1	0.0048
Estimated GFR (mL/min/1.73/m^2)	81.5 ± 20.9	68.2 ± 22.1	0.0154
BNP (pg/mL)	11.3(4.4 – 48.4)	158 (53.8 – 308)	<0.0001
Echocardiography			
IVSD (mm)	11.5 ± 4.1	11.6 ± 3.6	NS
LVPWD (mm)	10.5 ± 2.3	11.2 ± 2.8	NS
LVEDD (mm)	47 ± 6.7	48 ± 9.6	NS
LVEF (%)	68 ± 11	63 ± 11	NS
LAD (mm)	36 ± 6.6	43 ± 9.8	0.0101
E/A ratio	1.06 ± 0.5	0.89 ± 0.4	NS
E wave DCT (ms)	225 ± 49	228 ± 140	NS
^{123}I-MIBG imaging			
Early H/M ratio	2.13 ± 0.3	1.93 ± 0.3	0.0088
Delayed H/M ratio	2.30 ± 0.3	1.84 ± 0.3	<0.0001
WR (%)	10.1 ± 6.8	29.4 ± 15.4	<0.0001
Medications			
ACE inhibitors and/or ARBs	2 (10%)	53 (56%)	0.0002
β -blockers	1 (5%)	37 (39%)	0.0031
Ca-channel blockers	3 (15%)	23 (24%)	NS
Loop diuretics	0 (0%)	39 (41%)	0.0004
Spironolactone	0 (0%)	14 (15%)	NS
Statins	2 (10%)	10 (11%)	NS
Digoxin	0 (0%)	22 (23%)	0.0160

HFPEF, heart failure with preserved ejection fraction; NYHA, New York Heart Association; GFR, glomerular filtration rate; BNP, brain natriuretic peptide; IVSD, intra ventricular septal dimension; LVPWD, left ventricular posteriol dimension; LVEDD, left ventricular end-diastolic dimension; LVEF, left ventricular ejection fraction; LAD, left atrial dimension; DCT, deceleration time; ^{123}I-MIBG, iodine-123 meta-iodobenzylguanidine; H/M, heart to mediastinum; WR, washout rate; ACE, angiotensin-converting enzyme; ARB, angiotensin II receptor blocker; NS, no significance.

Table 2. Comparisons of clinical characteristics between patients with low and high values of ^{123}I-MIBG washout rate

	Low WR (< 25.2%) group n = 48	High WR (≥ 25.2%) group n = 46	p Value
Age (y)	62 ± 15	67 ± 14	NS
Gender (male/female)	28/20	26/20	NS
NYHA functional Class (I/II/III)	23/23/2	3/28/15	<0.0001
Hypertension	24 (50%)	24 (52%)	NS
Hyperlipidemia	8 (17%)	9 (20%)	NS
Diabetes mellitus	3 (6%)	14 (30%)	0.0023
Current smoker	8 (17%)	11 (24%)	NS
Etiology			
Dilated cardiomyopathy	12 (25%)	7 (15%)	-
Ischemic heart failure	6 (13%)	8 (17%)	-
Valvular heart disease	10 (21%)	13 (28%)	-
Hypertensive heart disease	2 (4%)	4 (9%)	-
Arrhythmogenic	10 (21%)	7 (15%)	-
Others	7 (15%)	8 (17%)	-
Blood examination			
Sodium (mEq/L)	141 ± 2.2	141 ± 3.2	NS
Uric acid (mg/dL)	6.1 ± 2.0	6.2 ± 2.2	NS
Estimated GFR (mL/min/1.73/m^2)	74.3± 22.7	61.8 ± 19.7	0.0053
BNP (pg/mL)	79.8 (27.9 – 140)	202 (120 – 459)	<0.0001
H-FABP (ng/mL)	4.9 ± 4.7	5.7 ± 4.7	NS
Echocardiography			
IVSD (mm)	11.1 ± 3.4	12.1 ± 3.8	NS
LVPWD (mm)	10.9 ± 2.6	11.5 ± 3.0	NS
LVEDD (mm)	48 ± 9.8	49 ± 9.4	NS
LVEF (%)	62 ± 11	65 ± 11	NS
LAD (mm)	41 ± 8.8	44 ± 11	NS
E/A ratio	0.95 ± 0.4	0.83 ± 0.4	NS
E wave DCT (ms)	203 ± 55	251 ± 187	NS
^{123}I-MIBG imaging			
Early H/M ratio	2.00 ± 0.3	1.86 ± 0.4	0.0416
Delayed H/M ratio	2.00 ± 0.3	1.67 ± 0.3	<0.0001
WR(%)	18.2 ± 6.9	40.9 + 13.2	<0.0001
Medications			
ACE inhibitors and/or ARBs	24 (50%)	29 (63%)	NS
β -blockers	15 (31%)	22 (48%)	NS
Ca-channel blockers	11 (23%)	12 (26%)	NS
Loop diuretics	18 (38%)	21 (46%)	NS
Spironolactone	5 (10%)	9 (20%)	NS
Statins	2 (4%)	8 (17%)	0.0376
Digoxin	11 (23%)	11 (24%)	NS

H-FABP, heart-type fatty acid binding protein. Other abbreviations see in Table 1.

Table 3. Results of the univariate Cox proportional hazard analysis

Variables	HR	95% CI of HR	p Value
Age (per 1year increase)	1.032	0.999-1.067	NS
NYHA functional Class I, II vs. III	3.869	1.767-8.469	0.007
Sodium*	0.655	0.439-0.979	0.0389
Uric acid*	2.143	1.361-3.372	0.001
Estimated GFR*	0.588	0.387-0.915	0.0172
$Log_{10}BNP$*	1.553	1.030-2.340	0.0353
LAD*	1.928	1.349-2.732	0.0003
LVEF*	1.057	0.715-1.539	NS
WR*	1.969	1.398-2.754	<0.0001

*: per 1 SD increase

HR, hazard ratio; CI, confidence interval. Other abbreviations see in Table 1.

Table 4. Results of the multivariate Cox proportional hazard analysis

Variables	HR	95% CI of HR	p Value
NYHA functional Class I, II vs. III	0.632	0.153-2.608	NS
Sodium*	0.801	0.512-1.249	NS
Uric acid*	1.770	1.025-3.059	0.0404
Estimated GFR*	1.022	0.640-1.653	NS
$Log_{10}BNP$*	1.167	0.675-2.016	NS
LAD*	1.205	0.772-1.888	NS
WR*	1.688	1.016-2.794	0.0437

*: per 1SD increase

Other abbreviations see in Table 1 and 3

Fig. 1.

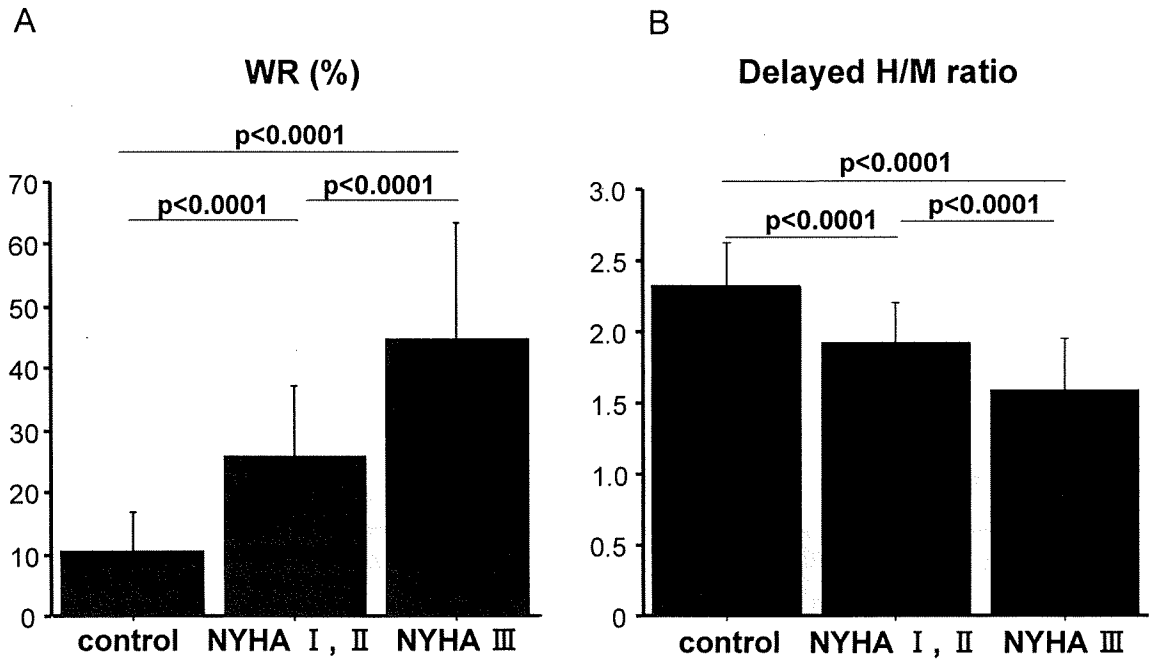
A
WR (%)
p<0.0001
p<0.0001
p<0.0001
70
60
50
40
30
20
10
0
control
NYHA Ⅰ, Ⅱ
NYHA Ⅲ
B
Delayed H/M ratio
p<0.0001
p<0.0001
p<0.0001
3.0
2.5
2.0
1.5
1.0
0.5
0
control
NYHA Ⅰ, Ⅱ
NYHA Ⅲ

Fig. 2.

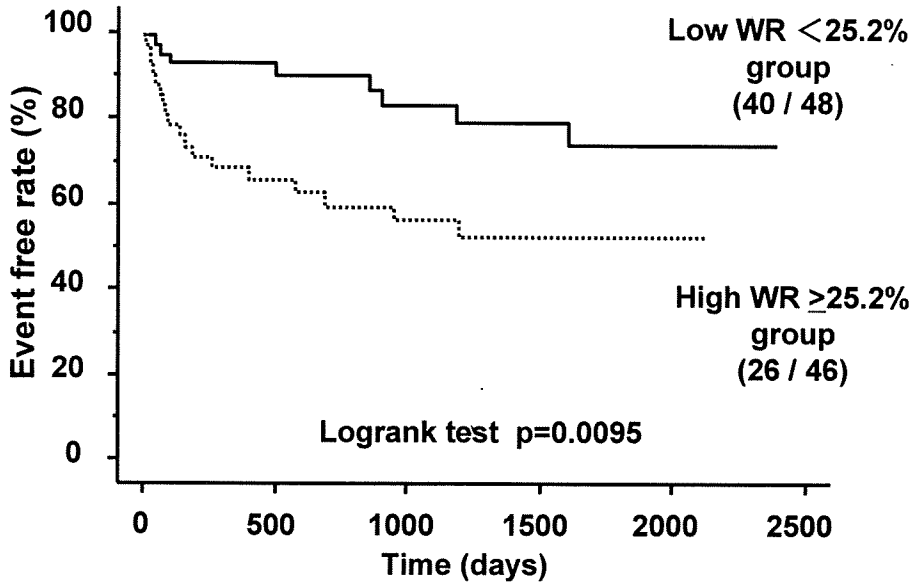
Event free rate (%)
100
80
60
40
20
0
0
500
1000
1500
2000
2500
Time (days)
Low WR <25.2%
group
(40 / 48)
High WR ≥25.2%
group
(26 / 46)
Logrank test p=0.0095

Fig. 3.

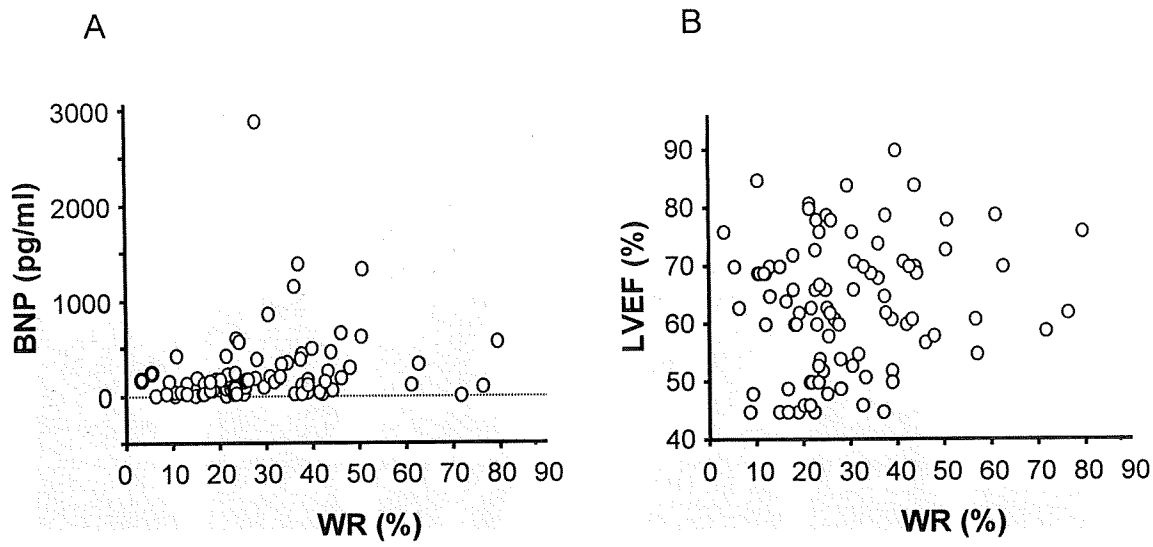
A
B
BNP (pg/ml)
3000
2000
1000
0
0 10 20 30 40 50 60 70 80 90
WR (%)
LVEF (%)
90
80
70
60
50
40
0 10 20 30 40 50 60 70 80 90
WR (%)

Fig. 4.

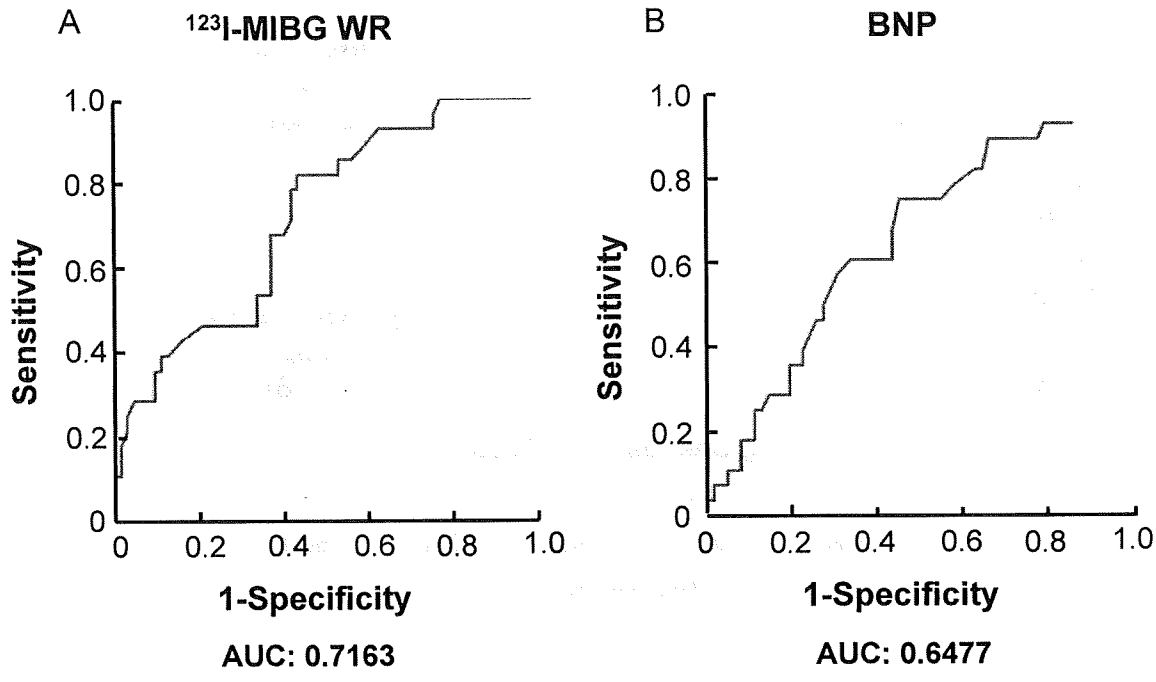
A
123I-MIBG WR
Sensitivity
1.0
0.8
0.6
0.4
0.2
0
0 0.2 0.4 0.6 0.8 1.0
1-Specificity
AUC: 0.7163
B
BNP
Sensitivity
1.0
0.8
0.6
0.4
0.2
0
0 0.2 0.4 0.6 0.8 1.0
1-Specificity
AUC: 0.6477

Fig. 4.

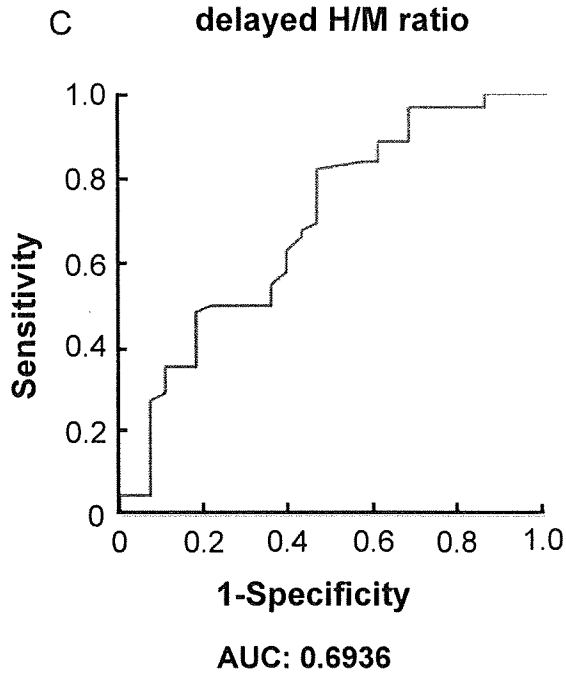
C
delayed H/M ratio
1.0
0.8
0.6
0.4
0.2
0
Sensitivity
0
0.2
0.4
0.6
0.8
1.0
1-Specificity
AUC: 0.6936

Research article

Cardiac fibroblasts are essential for the adaptive response of the murine heart to pressure overload

Norifumi Takeda,[1] Ichiro Manabe,[1,2,3] Yuichi Uchino,[1] Kosei Eguchi,[1] Sahohime Matsumoto,[1] Satoshi Nishimura,[1,3] Takayuki Shindo,[3,4] Motoaki Sano,[3,5] Kinya Otsu,[6] Paige Snider,[7] Simon J. Conway,[7] and Ryozo Nagai[1,2,8,9]

[1]Department of Cardiovascular Medicine and [2]Global COE Program, Graduate School of Medicine, University of Tokyo, Tokyo, Japan. [3]PRESTO, Japan Science and Technology Agency, Saitama, Japan. [4]Department of Organ Regeneration, Shinshu University Graduate School of Medicine, Nagano, Japan. [5]Department of Regenerative Medicine and Advanced Cardiac Therapeutics, Keio University School of Medicine, Tokyo, Japan. [6]Department of Cardiovascular Medicine, Osaka University Graduate School of Medicine, Suita, Japan. [7]Riley Heart Research Center, Herman B Wells Center for Pediatric Research, Indiana University of Medicine, Indianapolis, Indiana, USA. [8]Comprehensive Center of Education and Research for Chemical Biology of the Diseases, Graduate School of Medicine, University of Tokyo, Tokyo, Japan. [9]Translational Research Center, University of Tokyo Hospital, Tokyo, Japan.

Fibroblasts, which are the most numerous cell type in the heart, interact with cardiomyocytes in vitro and affect their function; however, they are considered to play a secondary role in cardiac hypertrophy and failure. Here we have shown that cardiac fibroblasts are essential for the protective and hypertrophic myocardial responses to pressure overload in vivo in mice. Haploinsufficiency of the transcription factor–encoding gene Krüppel-like factor 5 (*Klf5*) suppressed cardiac fibrosis and hypertrophy elicited by moderate-intensity pressure overload, whereas cardiomyocyte-specific *Klf5* deletion did not alter the hypertrophic responses. By contrast, cardiac fibroblast–specific *Klf5* deletion ameliorated cardiac hypertrophy and fibrosis, indicating that KLF5 in fibroblasts is important for the response to pressure overload and that cardiac fibroblasts are required for cardiomyocyte hypertrophy. High-intensity pressure overload caused severe heart failure and early death in mice with *Klf5*-null fibroblasts. KLF5 transactivated *Igf1* in cardiac fibroblasts, and IGF-1 subsequently acted in a paracrine fashion to induce hypertrophic responses in cardiomyocytes. *Igf1* induction was essential for cardioprotective responses, as administration of a peptide inhibitor of IGF-1 severely exacerbated heart failure induced by high-intensity pressure overload. Thus, cardiac fibroblasts play a pivotal role in the myocardial adaptive response to pressure overload, and this role is partly controlled by KLF5. Modulation of cardiac fibroblast function may provide a novel strategy for treating heart failure, with KLF5 serving as an attractive target.

Introduction

Myocardial hypertrophy is an essential adaptive process through which the heart responds to various mechanophysical, metabolic, and genetic stresses. However, the hypertrophy induced by sustained overload eventually leads to contractile dysfunction and heart failure through mechanisms that remain poorly understood (1). In addition to enlargement of individual cardiomyocytes, the hypertrophied myocardium exhibits complex structural remodeling that involves rearrangement of the muscle fibers, interstitial fibrosis, accumulation of extracellular matrix, and angiogenesis (2, 3), which implies that the non-muscle cells residing in the interstitium likely play important roles in both cardiac hypertrophy and heart failure. In fact, cells other than cardiomyocytes account for approximately 70% of the total cell number in the heart, with the majority being fibroblasts (4, 5). In addition to extracellular matrix proteins (e.g., collagens), cardiac fibroblasts produce a variety of growth factors that likely mediate an interplay between cardiac fibroblasts and cardiomyocytes. For instance, several humoral factors secreted by cardiac fibroblasts, including cardiotrophin-1 (6), endothelin-1 (7), IL-6 (8), periostin (POSTN) (9), and leukemia inhibitory factor (10), have been shown to induce hypertrophic responses in cultured cardiomyocytes. Cardiac fibroblasts also promote proliferation of cardiomyocytes through paracrine interactions in developing hearts (11). And very recently it was shown that inhibition of a fibroblast-selective miRNA ameliorated cardiac fibrosis, hypertrophy, and dysfunction, suggesting that fibroblasts play a detrimental role in cardiac remodeling (12). Still, the precise function of cardiac fibroblasts during adaptive responses of the myocardium remains unclear (2).

Members of the Krüppel-like factor (KLF) family of transcription factors are important regulators of development, cellular differentiation and growth, and the pathogenesis of various diseases, including cancer and cardiovascular disease (13). We previously used *Klf5*$^{+/-}$ mice to show that KLF5 is required for cardiac hypertrophy and fibrosis in response to continuous infusion of angiotensin II (AII) (14, 15). In primary cultured cardiac fibroblasts, KLF5 directly controls transcription of *Pdgfa*, encoding platelet-derived growth factor A (PDGF-A) (14), which is known to be involved in tissue remodeling and wound healing (16–19). The precise role played by KLF5 in cardiac hypertrophy and heart failure remains unclear, however.

In the present study, we developed conditional *Klf5*-knockout mouse lines to examine the cell type–specific functions of KLF5 in cardiac hypertrophy and heart failure. While cardiomyocyte-specific deletion of *Klf5* did not alter the hypertrophic responses

Conflict of interest: The authors have declared that no conflict of interest exists.
Citation for this article: *J. Clin. Invest.* 120:254–265 (2010). doi:10.1172/JCI40295.

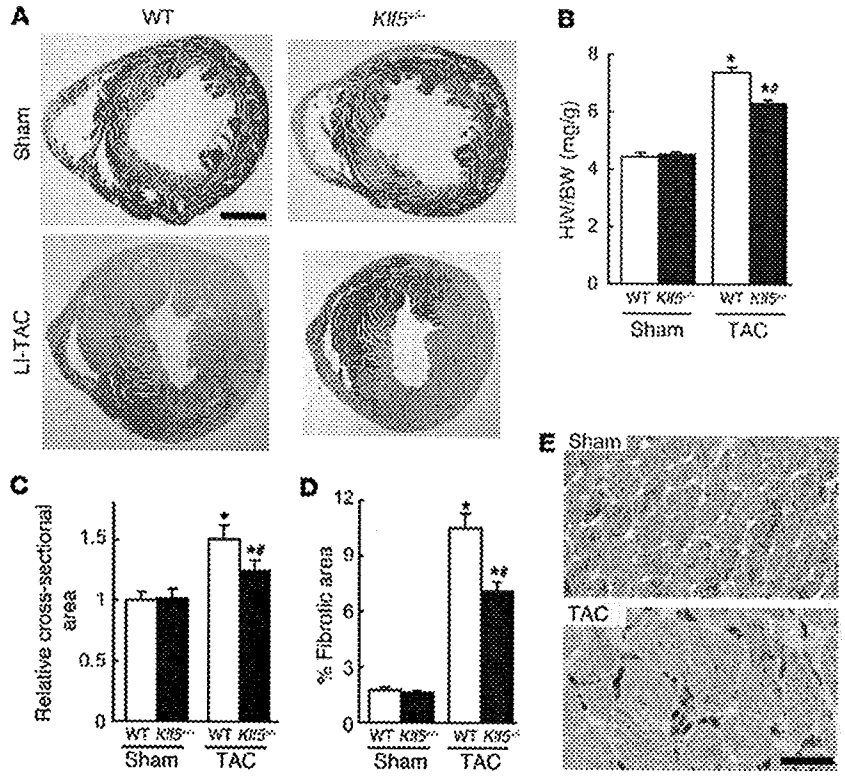

Figure 1
KLF5 is essential for pressure overload–induced hypertrophy. (**A–D**) *Klf5*$^{+/-}$ and wild-type mice were subjected to LI-TAC or sham operation. (**A**) Representative low-magnification views of H&E-stained heart sections from WT and *Klf5*$^{+/-}$ mice 2 weeks after the operations. Scale bar: 1 mm. (**B** and **C**) Heart weight/body (HW/BW) weight ratios (**B**) and relative cross-sectional areas of cardiomyocytes (**C**) from wild-type and *Klf5*$^{+/-}$ hearts. (**D**) Fractional areas of fibrosis in cross sections of hearts as determined by elastic picrosirius red staining. $^{*}P < 0.01$ versus sham control of the same genotype; $^{\#}P < 0.05$ versus wild-type subjected to TAC. $n = 7$. (**E**) Expression of KLF5 in normal and hypertrophied hearts 4 days after LI-TAC. Cells were double stained for KLF5 (brown) and a cardiomyocyte marker, αMHC (red); nuclei were counterstained in blue. Scale bar: 20 μm.

to pressure overload, cardiac fibroblast–specific deletion of *Klf5* ameliorated cardiac hypertrophy in a moderate-intensity pressure overload model, indicating that fibroblasts are essential for hypertrophic responses of the myocardium. Notably, however, cardiac fibroblast–specific *Klf5*-knockout mice developed severe heart failure when subjected to high-intensity pressure overload, suggesting cardiac fibroblasts have a cardioprotective function. We further demonstrated that KLF5 controls expression of IGF-1, which mediates the interplay between cardiomyocytes and fibroblasts. These data provide compelling evidence that cardiac fibroblasts play a pivotal role in the adaptive response of the myocardium.

Results

KLF5 plays an important role in pressure overload–induced cardiac hypertrophy. To analyze KLF5's function in cardiac adaptive responses, we first established models of pressure overload–induced cardiac hypertrophy using transverse aortic constriction (TAC). By applying a low-intensity TAC (LI-TAC) for 2 weeks, we were able to induce cardiac hypertrophy with preserved cardiac systolic function, while application of high-intensity TAC (HI-TAC) induced severe myocardial dysfunction and LV dilation (Supplemental Figures 1 and 2; supplemental material available online with this article; doi:10.1172/JCI40295DS1). The survival rates in the LI- and HI-TAC groups were 100% and 90%, respectively, after 2 weeks, which suggests that the LI-TAC model induces adaptive hypertrophy, while in the HI-TAC model, the adaptive response fails to protect against the severe pressure overload and enable maintenance of cardiac function.

When we examined the involvement of KLF5 in cardiac hypertrophy using the LI-TAC model, we found that cardiac expression of KLF5 was increased by LI-TAC (Supplemental Figure 3) and that LI-TAC–induced cardiac hypertrophy and fibrosis was diminished in *Klf5*$^{+/-}$ mice (Figure 1 and Supplemental Figure 4). Moreover, expression of 4 fibrosis-related genes, *Col1a1*, *Fn1*, *Ctgf*, and *Spp1*, was significantly suppressed in *Klf5*$^{+/-}$ mice (Supplemental Figure 4). Thus KLF5 appears to play a critical role in pressure overload–induced cardiac hypertrophy and fibrosis.

Cardiomyocyte-specific deletion of Klf5 does not affect pressure overload–induced cardiac hypertrophy. We found that *Klf5* is mainly expressed in fibroblasts (Supplemental Figure 3C), which suggests that its function in fibroblasts might contribute to the phenotypes seen in *Klf5*$^{+/-}$ mice. To test this idea, we generated several conditional *Klf5*-knockout mouse lines (Supplemental Figure 5). Homozygous *Klf5*-floxed (*Klf5*$^{fl/fl}$) mice appeared normal, and expression of *Klf5* was unaltered (data not shown). The *Klf5*$^{fl/fl}$ mice were then crossed with cardiomyocyte-specific Cre transgenic mice (*αMHC-Cre*) (20). In cardiomyocytes from adult cardiomyocyte-specific *Klf5*-knockout (*Klf5*$^{fl/fl}$;*αMHC-Cre*) mice, which were homozygous for both floxed *Klf5* and the *αMHC-Cre* transgene, approximately 70% of the *Klf5* gene was deleted (Supplemental Figure 6). When *Klf5*$^{fl/fl}$;*αMHC-Cre* mice and control *Klf5*$^{fl/fl}$ mice were subjected to LI-TAC, there were no differences in cardiac structure or function, or gene expression, between the 2 groups (Figure 2 and Supplemental Figure 7), which means that the level of *Klf5* deletion obtained in *Klf5*$^{fl/fl}$;*αMHC-Cre* mice did not affect the hypertrophic response to TAC.

Cardiac fibroblast–specific deletion of Klf5 reduces hypertrophic and fibrotic responses. We then analyzed the function of KLF5 in cardiac fibroblasts using a transgenic mouse line in which Cre recombinase was driven by a 3.9-kb mouse *Postn* promoter (21, 22), which is restricted to the non-myocyte lineage in the neonatal heart (P. Snider and S.J. Conway, unpublished observations). Periostin, which is encoded by *Postn*, is not normally expressed in either the

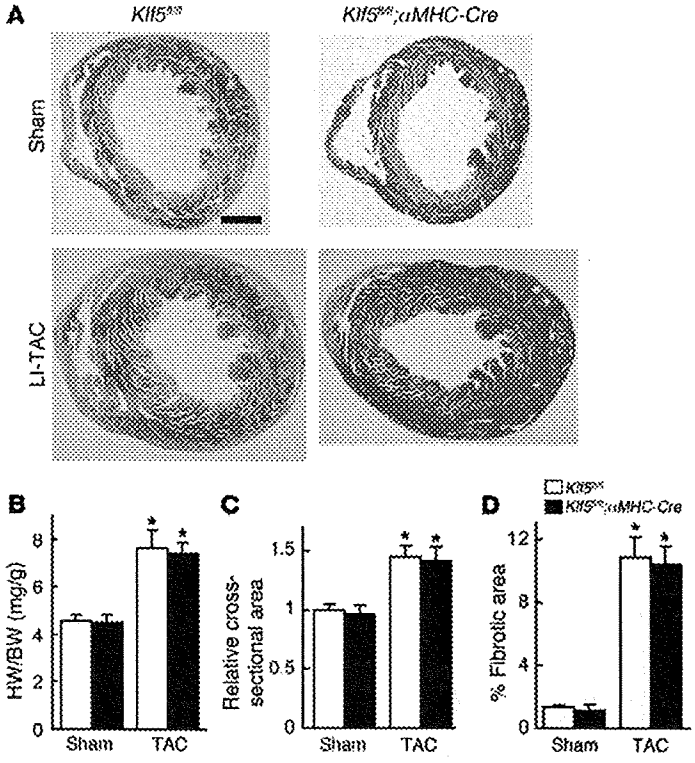

Figure 2
Cardiomyocyte-specific deletion of *Klf5* did not alter pressure overload–induced hypertrophy. *Klf5*$^{fl/fl}$ and *Klf5*$^{fl/fl}$;*αMHC-Cre* mice were subjected to LI-TAC or sham operation. (**A**) Representative low-magnification views of H&E-stained heart sections 2 weeks after LI-TAC. Scale bar: 1 mm. (**B** and **C**) Heart weight/body weight ratios (**B**) and relative cross-sectional areas of cardiomyocytes normalized to those obtained from *Klf5*$^{fl/fl}$ mice subjected to sham operations (**C**). (**D**) Fractional areas of fibrosis. $^*P < 0.01$ versus sham control of the same genotype. $n = 7$.

normal or pathological cardiomyocyte lineage (23), but is induced in cardiac fibroblasts by TAC (9, 24, 25). The activity of Cre recombinase in the *Postn-Cre* mice was examined after they were crossed with *R26RstoplacZ* indicator mice (26). Although only a few β-galactosidase$^+$ cells were found in the heart under basal conditions, LI-TAC induced robust *lacZ* expression in fibrotic areas in hearts from *R26RstoplacZ;Postn-Cre* mice (Figure 3A and Supplemental Figure 8). As expected, *lacZ* expression was not detected in either cardiomyocytes or ECs (Supplemental Figure 8).

We then used flow cytometry to further analyze expression of β-galactosidase in populations enriched in either cardiomyocytes or non-myocytes isolated from *R26RstoplacZ;Postn-Cre* mice subjected to LI-TAC (Supplemental Figure 9). β-Galactosidase$^+$ cells were not found in the cardiomyocyte population. Moreover, β-galactosidase$^+$ cells isolated from the non-myocyte population expressed a fibroblast-specific marker, discoidin domain receptor 2 (*Ddr2*), but not the cardiomyocyte-specific marker αMHC (*Myh6*) or the endothelial marker VE-cadherin (*Cdh5*), which supports the notion that β-galactosidase$^+$ cells are fibroblasts.

Klf5$^{fl/fl}$ mice were then bred with the *Postn-Cre* mice to generate *Klf5*$^{fl/fl}$*;Postn-Cre* mice. These animals were born with no apparent abnormalities and were healthy into adulthood. To examine the efficacy of Cre-mediated deletion of *Klf5* in each cell type, we isolated cardiomyocytes, cardiac fibroblasts, and ECs from adult mice. Cardiomyocytes were isolated using the Langendorff perfusion method (27). Fibroblasts and ECs were sorted from non-myocyte-enriched cell populations using anti-Thy1 antibody for fibroblasts (11, 28) and anti-CD31 for ECs. Because Thy1 is also expressed in T lymphocytes, CD3$^-$ cells were analyzed for surface expression of Thy1 and CD31 (Figure 3B). When the mRNA expression of cell type–specific lineage markers was analyzed, *Myh6* was found to be expressed only in cardiomyocytes, while *Ddr2* was expressed only in Thy1$^+$CD31$^-$CD3$^-$ cells and *Cdh5* only in Thy1$^-$CD31$^+$CD3$^-$ cells (Figure 3C), which indicates that Thy1$^+$CD31$^-$CD3$^-$ cells were fibroblasts. Approximately 72% of the *Klf5* gene was deleted in Thy1$^+$CD31$^-$CD3$^-$ fibroblasts isolated from *Klf5*$^{fl/fl}$*;Postn-Cre* mice subjected to LI-TAC for 2 weeks, whereas only 4% was deleted in the sham-operated mice (Figure 3D). No *Klf5* deletion was observed in cardiomyocytes or ECs. Moreover, *Cre* mRNA was selectively expressed in Thy1$^+$ fibroblasts, as was endogenous *Postn* mRNA, which is consistent with fibroblast-specific Cre-mediated deletion by *Postn-Cre* (Supplemental Figure 10).

We further analyzed expression of *Klf5* mRNA in each cell type in mice subjected to either the sham operation or LI-TAC (Figure 3E). In sham-operated hearts, levels of *Klf5* expression were higher in Thy1$^+$ fibroblasts than in cardiomyocytes or ECs and did not differ between *Klf5*$^{fl/fl}$ and *Klf5*$^{fl/fl}$*;Postn-Cre* mice. LI-TAC markedly increased *Klf5* expression in fibroblasts (approximately 4-fold) and moderately increased it in cardiomyocytes in *Klf5*$^{fl/fl}$ mice. While *Klf5* expression was clearly reduced in fibroblasts from *Klf5*$^{fl/fl}$*;Postn-Cre*, as compared with *Klf5*$^{fl/fl}$ mice, it was not altered in cardiomyocytes, which is again consistent with fibroblast-specific deletion of *Klf5*.

LI-TAC induced less cardiac interstitial fibrosis in *Klf5*$^{fl/fl}$*;Postn-Cre* mice than in control *Klf5*$^{fl/fl}$ mice, as expected (Figure 4, A–C), and expression of fibrosis-related factors such as *Col1a1*, *Fn1*, *Ctgf*, and *Spp1* was reduced (Supplemental Figure 11A). In addition to fibrosis, increases in heart weight/body weight ratios, echocardiographic LV wall thickness, and cardiomyocyte cross-sectional area were smaller in *Klf5*$^{fl/fl}$*;Postn-Cre* mice than *Klf5*$^{fl/fl}$ mice (Figure 4, D–F). Moreover, expression levels of hypertrophy-related genes such as *Nppa*, which encodes atrial natriuretic peptide (ANP), and *Myh7*, which encodes β–myosin heavy chain, were lower in *Klf5*$^{fl/fl}$*;Postn-Cre* than *Klf5*$^{fl/fl}$ mice (Figure 4G), indicating suppression of hypertrophic responses. These phenotypes clearly demonstrate that not only is KLF5 expressed in cardiac fibroblasts essential for fibrosis, it is also important for mediating subsequent cardiomyocyte hypertrophy.

IGF-1 controlled by KLF5 mediates hypertrophic responses. We next investigated the mechanisms by which KLF5 expressed in fibroblasts controls hypertrophy of cardiomyocytes. Because earlier studies have suggested there are paracrine interactions between cardiomyocytes and fibroblasts (2, 3), we hypothesized that KLF5 might directly control the expression of paracrine factors in fibroblasts. To test that idea, we cultured cardiomyocytes in medium conditioned by cardiac fibroblasts transfected with either siRNA against KLF5 (29) or control siRNA (Figure 5A). We found that the medium conditioned by KLF5 knockdown fibroblasts was

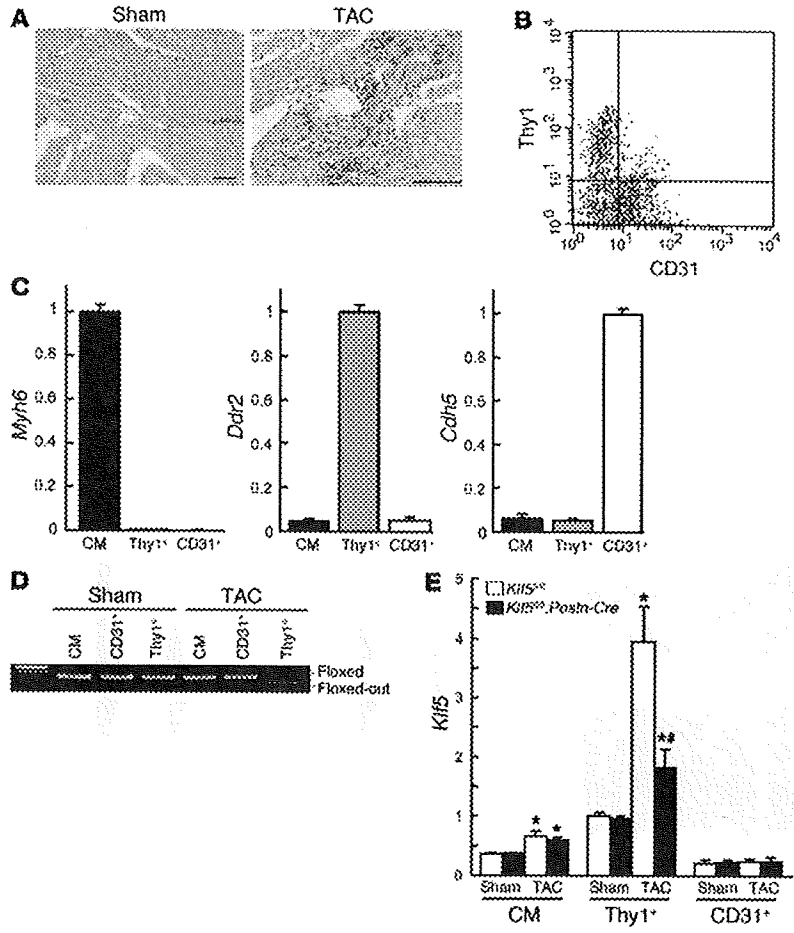

Figure 3

Fibroblast-specific deletion of *Klf5* in *Klf5$^{fl/fl}$;Postn-Cre* mice. (**A**) Fibroblast-specific deletion of the floxed region in *Postn-Cre* mice was examined using *R26RstoplacZ* indicator mice. *LacZ* expression was visualized using X-gal. Scale bars: 100 μm. (**B**) CD3$^-$ cells within non-myocyte-enriched cell populations isolated from adult hearts were analyzed for surface expression of the fibroblast marker Thy1 and the endothelial marker CD31. (**C**) Relative expression levels of cell-lineage markers in adult cardiomyocytes (CM) isolated using the Langendorff perfusion method, and in Thy1$^+$CD31$^-$CD3$^-$ (Thy1$^+$) and Thy1$^-$CD31$^+$CD3$^-$ (CD31$^+$) cells sorted from non-myocyte-enriched populations as shown in **B**. *Myh6* (encoding αMHC), *Ddr2* (encoding discoidin domain receptor 2), and *Cdh5* (encoding VE-cadherin) were used as markers for cardiomyocytes, fibroblasts, and ECs, respectively. The cells were isolated from 8-week-old mice subjected to sham operations. (**D**) Competitive PCR analysis for quantitation of Cre-mediated recombination of the *Klf5* gene region in adult cardiomyocytes, CD31$^+$ ECs, and Thy1$^+$ fibroblasts isolated from *Klf5$^{fl/fl}$* and *Klf5$^{fl/fl}$;Postn-Cre* mice 2 weeks after either the sham or LI-TAC operation. Competitive PCR was performed as shown in Supplemental Figure 6B. (**E**) Relative expression levels of *Klf5* mRNA in adult cardiomyocytes, Thy1$^+$ fibroblasts, and CD31$^+$ ECs isolated from *Klf5$^{fl/fl}$* and *Klf5$^{fl/fl}$;Postn-Cre* mice as shown in **B** 5 days after either sham operation or LI-TAC. Expression levels of *Klf5* mRNA were assessed using real-time PCR and normalized to those of 18s rRNA, after which they were further normalized to the levels in Thy1$^+$ cells isolated from *Klf5$^{fl/fl}$* mice subjected to the sham operation. $^*P < 0.01$ versus sham control of the same genotype in the same cell lineage group; $^\#P < 0.01$ versus *Klf5$^{fl/fl}$* mice subjected to LI-TAC in the same cell lineage group.

less able to induce cardiomyocyte hypertrophy and ANP secretion than medium conditioned by control cells (Figure 5, B–D), suggesting that, in fibroblasts, KLF5 does indeed control production of paracrine factors that induce hypertrophic responses in cardiomyocytes. Similarly, Thy1$^+$ cardiac fibroblasts isolated from *Klf5$^{fl/fl}$;Postn-Cre* mice subjected to LI-TAC were less able to induce cardiomyocyte hypertrophy than Thy1$^+$ cells from *Klf5$^{fl/fl}$* mice (Supplemental Figure 12).

To identify the paracrine factor genes targeted by KLF5, we compared genome-wide gene expression profiles for the left ventricle in wild-type mice subjected to the sham operation and those subjected LI-TAC; and in *Klf5$^{fl/fl}$* and *Klf5$^{fl/fl}$;Postn-Cre* mice subjected to LI-TAC (Supplemental Table 1). Thereafter, expression levels were verified by real-time PCR. We screened for genes encoding secreted proteins whose expression levels were significantly increased by LI-TAC in wild-type mice and were lower in *Klf5$^{fl/fl}$;Postn-Cre* than *Klf5$^{fl/fl}$* mice. Among the 11 genes that met these criteria, 6 were preferentially expressed in cardiac fibroblasts, as compared with cardiomyocytes (Supplemental Table 1), and included 2 growth factor genes, *Igf1* and *Tgfb3*, encoding IGF-1 and TGF-β3, and *Postn*, encoding periostin. While knocking down KLF5 significantly reduced expression of *Igf1* in cultured fibroblasts (Figure 6A), expression levels of *Tgfb3* and *Postn* were not altered (Supplemental Figure 13), suggesting that KLF5 might directly control *Igf1* transcription. Moreover, *Igf1* expression was highly enriched in fibroblasts (Figure 6B). IGF-1 reportedly promotes cardiac growth and improves cardiac function in patients with LV dysfunction and advanced heart failure (30–32). We therefore further analyzed *Igf1* as a likely downstream target of KLF5.

We found that upregulation of myocardial *Klf5* expression after LI-TAC preceded the induction of *Igf1* (Figure 6C). Levels of both *Klf5* and *Igf1* expression were reduced in *Klf5$^{fl/fl}$;Postn-Cre* mice, as compared with those in *Klf5$^{fl/fl}$* mice, during the 2-week observation period following the LI-TAC operation. The *Igf1* promoter contains a KLF-binding motif (CCCCACCCAC) at −53 bp, which, in the rat, is reportedly important for promoter activity and bound by an as-yet-unidentified transcription factor (Figure 6D) (33). Reporter analysis of the *Igf1* promoter showed that KLF5 transactivated this promoter, but KLF15, which is expressed in cardiomyocytes and cardiac fibroblasts (34, 35), failed to do so, and mutation within the potential KLF5-binding motif abolished KLF5-dependent transactivation (Figure 6D). ChIP assays confirmed that KLF5 bound to the *Igf1* promoter (Figure 6E). As reported (30–32), IGF-1 induced hypertrophy in cultured cardiomyocytes (Supplemental Figure 14A), and inhibition of IGF-1 using a neutralizing antibody significantly suppressed cardiomyocyte hypertrophy induced by the fibroblast-conditioned medium (Figure 6F). Taken together, the results so far demonstrate that KLF5 directly regulates expression of *Igf1*, which appears to be a major cardiotrophic factor secreted by fibroblasts.

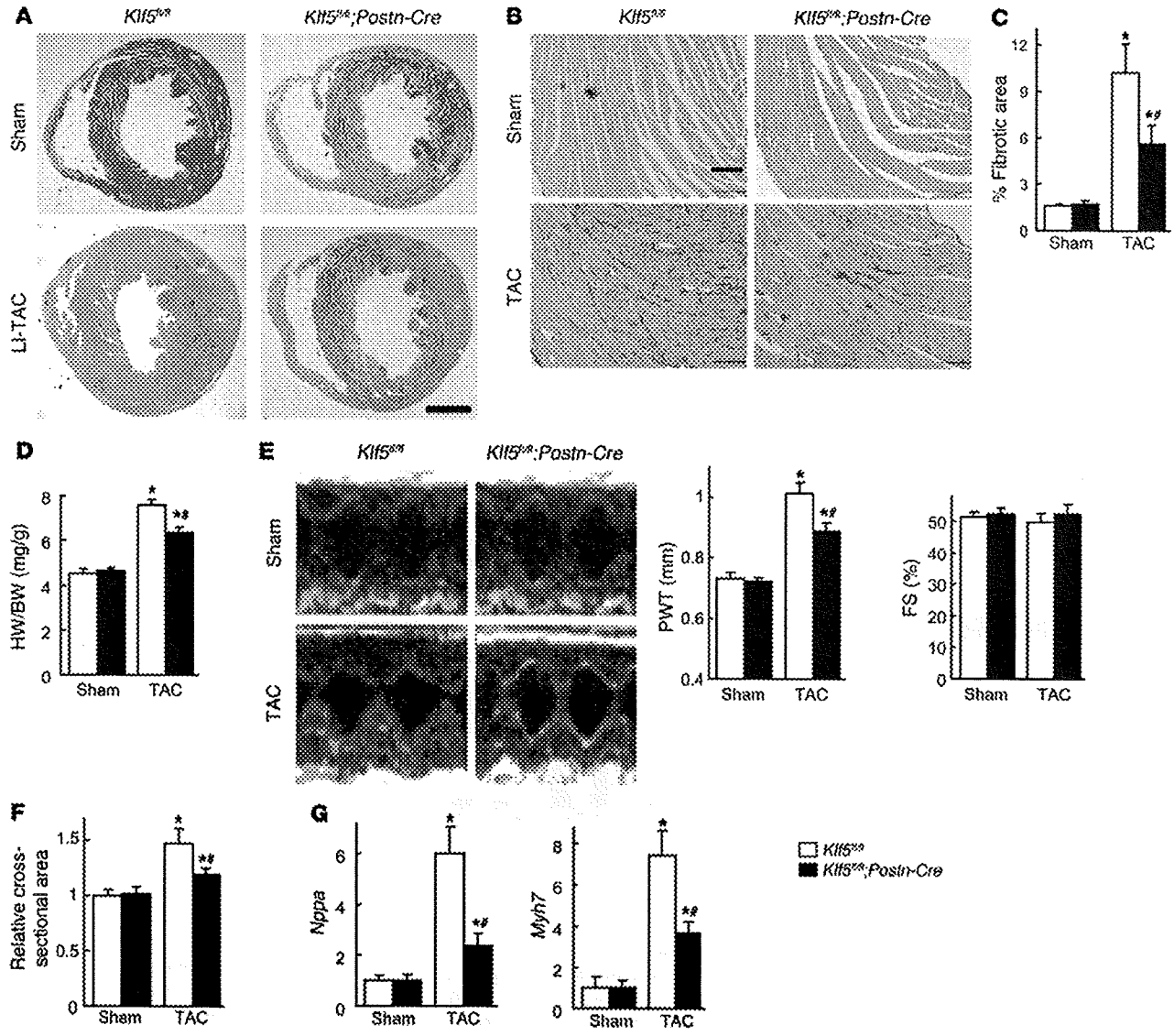

Figure 4

Fibroblast-specific deletion of *Klf5* attenuates cardiac hypertrophy and fibrosis after TAC. *Klf5*$^{fl/fl}$ and *Klf5*$^{fl/fl}$;*Postn-Cre* mice were subjected to LI-TAC or sham operation. (**A**) Representative low-magnification views of H&E-stained heart sections 2 weeks after the operations. Scale bar: 1 mm. The bottom-left panel was composited from 2 photographs of the same section. (**B**) Representative elastic picrosirius red–stained sections and fibrotic areas. Scale bars: 100 μm. (**C**) Fibrotic areas. (**D**) Heart weight/body weight ratios 2 weeks after the operations. (**E**) Echocardiographic analysis 2 weeks after the operations. (**F**) Relative cross-sectional areas of cardiomyocytes. (**G**) Relative expression levels of *Nppa* and *Myh7* mRNA. Expression levels of each gene were normalized to 18s ribosomal RNA levels and then further normalized with respect to those obtained with samples from *Klf5*$^{fl/fl}$ mice subjected to sham operation. $^{*}P < 0.01$ versus sham control of the same genotype; $^{\#}P < 0.01$ versus *Klf5*$^{fl/fl}$ subjected to TAC. $n = 7$.

We also found that the numbers of fibroblasts positive for BrdU incorporation following LI-TAC were significantly smaller in *Klf5*$^{fl/fl}$;*Postn-Cre* hearts than *Klf5*$^{fl/fl}$ hearts (Supplemental Figure 11B), which suggests that KLF5 may also be involved in modulating fibroblast proliferation, either autonomously (36–38) or by regulating autocrine/paracrine factors. Consistent with the latter, we found that IGF-1 induces fibroblast proliferation (Supplemental Figure 14B).

We previously reported that KLF5 also controls *Pdgfa*, which encodes PDGF-A, in response to angiotensin II (14, 39). At the same concentrations, PDGF-A was less able to induce cardiomyocyte hypertrophy than IGF-1 (Supplemental Figure 14A), though PDGF-A and IGF-1 similarly induced fibroblast proliferation (Supplemental Figure 14B). PDGF-A induced greater migration of fibroblasts in Boyden chamber assays than IGF-1 (Supplemental Figure 14C), suggesting PDGF-A is primarily involved in mediating the migration and proliferation of fibroblasts. Thus, among the paracrine factors controlled by KLF5, it appears to be a change in IGF-1 activity that is primarily responsible for the reduced cardiac hypertrophy observed in LI-TAC *Klf5*$^{fl/fl}$;*Postn-Cre* hearts.